Blue LD-pumped electro-optically Q-switched Pr:YLF visible laser with kilowatt-level peak power

Zixin Yang[a,b], Syed Zaheer Ud Din[a], Pengchao Wang[a], Chun Li[a], Zhiwei Lin[a], Jiancai Leng[b], Jie Liu[c], Lin Xu[d], Qi Yang[a,*], Xianghe Ren[a,*]

[a]*International School for Optoelectronic Engineering, Qilu University of Technology (Shandong Academy of Sciences), Jinan 250300, China*

[b]*School of Electronic and Information Engineering (Department of Physics), Qilu University of Technology (Shandong Academy of Sciences), Jinan 250300, China*

[c]*Shandong Provincial Engineering and Technical Center of Light Manipulations and Shandong Provincial Key Laboratory of Optics and Photonic Device, School of Physics and Electronics, Shandong Normal University, Jinan 250358, China*

[d]*Optoelectronics Research Centre, University of Southampton, Southampton SO17 1BJ, UK*

Corresponding author: shanshiyangqi@126.com; xhren101@hotmail.com;

Abstract: We report the generation of high energy visible pulsed beam from a blue LD-pumped electro-optically (EO) Q-switched Pr^{3+}:$LiYF_4$ (Pr:YLF) laser for the first time. The maximum pulse energy and highest peak power in our work perform excellent in the blue LD-pumped pulse visible lasers. The shortest pulse duration of 137 ns is obtained at the repetition rate of 100 Hz, corresponding to a single pulse energy of 260 μJ and peak power of 1.90 kW. Our research results indicate that the Pr:YLF crystal could be suitable for the generation of high energy Q-switched visible lasers. Meanwhile, we pave up a new way for the practical implementation of blue LD-pumped directly generate high energy Q-switched visible laser.

Keywords: EO Q-switched, Pr:YLF, Diode-pumped laser

Highlights

- Blue LD-pumped EO Q-switched Pr:YLF visible laser at 639 nm was demonstrated.
- Maximum pulse energy of 260 μJ and highest peak power of 1.90 kW were realized.
- Excellent beam quality visible pulsed laser was achieved.

1. Introduction

Visible lasers have gained much attraction in recent years due to their wide applications and requirements in various topical ranges, including optical data storage, medicine, complex reaction detection, display technology, underwater communications, and scientific research [1-4]. With the development of GaN semiconductor material, blue laser diodes (LDs) have become the dependable sources to pump rare-earth doped laser materials, such as Sm^{3+} [5], Tb^{3+} [6,7], Dy^{3+} [8], Pr^{3+} [9,10], and so on. Among them, Pr^{3+} is recognized as one of the most active ions for achieving efficient visible laser benefitting from its large emission section and four-level system visible transitions. In 2004, Richter et al. first reported a continuous-wave (CW) laser oscillation of Pr: YLF at 639.7 nm [9]. The output power of 1.8 mW with a slope efficiency of 24% was achieved in their work. In recent years, the output capability of GaN blue LD has increased rapidly, the corresponding level of visible laser output has been greatly improved. In 2018, H. Tanaka reported a high power CW Pr:YLF laser end pumped by blue laser diodes with the highest output power of 6.7 W at 640 nm and 3.7 W at 607 nm, respectively [10].

In the laser regime, pulsed lasers can provide much larger pulse energy or higher peak power for various applications that are not available for CW lasers. Short pulsed lasers can be obtained by modulating the Q-factor based on passively or actively Q-switched techniques. Recently, many research groups have made efforts to realize the short pulsed Pr:YLF visible laser using low-dimension materials as the passively Q-switched modulator [11-13]. In 2015, Wang et al. realized a passively Q-switched visible laser with Au nanorods as the optical modulator with the maximum output energy of 64.0 nJ and peak power of 0.34 W at 639 nm [11]. In 2017, Xu

et al. demonstrated a passively Q-switched diode-pumped Pr:YLF visible lasers using CdTe/CdS quantum dot as a saturable absorber (SA) at 640 nm. The maximum output energy was 320 nJ and the peak power was 1.4 W [12]. In 2019, Yang et al. employed MXene $Ti_3C_2T_x$ as the passively Q-switcher to realize the visible passively Q-switched laser at 639 nm with the pulse energy of 920 nJ and the peak power of 3.48 W [13]. In 2019, Kannari et al. applied Co^{2+}:$MgAl_2O_4$ (Co:MALO) as an SA to realize a passively Q-switched Pr:YLF visible laser with a pulse energy of 33.5 μJ and a peak power of 1084 W at 640 nm [14]. Recently, Kränkel et al. report a passively Q-switched Pr:YLF laser at 640 nm by used Co:MALO as an SA. In their work, the pulse energy of 1.3 μJ and the pulse width of 8.5 ns were realized from a 7.5 mm long cavity [15]. However, the passively Q-switched technique has a disadvantage in the uncontrolled pulse repetition rates and poor pulse instabilities. Moreover, the output energy of passively Q-switched Pr:YLF lasers was very low (generally in hundreds of nano joules), which seriously limited their practical applications. In contrast, the actively Q-switched techniques not only provide more stable modulation frequency but also have higher damage threshold than SAs. Kannari et al. [16] successfully realized the Pr:YLF pulsed lasers using the acousto-optic (AO) Q-switcher at visible band in 2014. In their work, the highest pulse energy was 3.3 μJ at 522 nm and 27 μJ at 639 nm, and the corresponding pulse width was 32 ns and 17 ns, respectively. In 2019, Jin et al. demonstrated a Q-switched single-longitudinal-mode Pr:YLF laser at 639.5 nm by using the AO modulator combined with the Fabry-Perot etalon. Correspondingly, the pulse energy was 3.94 μJ, with pulse width of 81.1 ns [17]. Compared with AO Q-switched technology, EO Q-switched technology could generate higher pulse energy and peak power based on faster switched speed, better hold-off ability, and higher extinction ratio. Unfortunately, the blue LD-pumped visible pulse laser achieved by EO Q-switched technology has not yet been reported.

In this paper, we report a blue LD-pumped pulsed Pr:YLF visible laser with the EO Q-switcher for the first time. In our experiment, the EO Q-switched laser could generate 137 ns, 260 μJ pulses with a peak power of 1.90 kW at a repetition rate of 100 Hz. The maximum pulse energy and highest peak power of EO Q-switched laser in this work perform excellent at 639 nm. Our work paves a new way of LD-pumped Pr:YLF lasers of the high energy pulsed visible laser generation.

2. Experimental setup

The experimental setup of the EO Q-switched laser is shown in Fig. 1, in which a simple plano-concave cavity with a length of 200 mm has been employed. The laser gain medium was an a-cut Pr:YLF crystal with 0.5 at.% doped. The cross section size of Pr:YLF crystal (Unioriental Optics Co., Ltd) was 3 mm × 3 mm, and the length was 6 mm. The absorption of anisotropic Pr:YLF crystal is polarization dependent, and the peak wavelength locates at 442 nm and 444 nm for the σ polarization absorption and π polarization absorption, respectively. Therefore, we chose two commercially single-emitter InGaN blue LDs (NUBM06, Nichia Corp.) emitting around 442 nm and 444 nm as the pump source for better absorption efficiency. Two LDs all emitted horizontally polarized light in which the 442 nm pump light was converted to vertically polarized light by the half-wave plate. The pump beams were combined with a polarization beam splitter (PBS), and then were focused into the Pr:YLF crystal by a focal lens with a focusing length of 75 mm. The pump beam radius was calculated to be about 69 μm inside Pr:YLF crystal and the pump Rayleigh length in laser crystal was about 3.4 cm. According to the ABCD propagation matrix method, the laser mode radius was calculated to be about 64 μm inside Pr:YLF crystal. Based on the above data, the overlap efficiency between pump and laser beams was approximately 92.8%. In the experiment, the pump absorption at 442 and 444 nm under the maximum pump power was about 69.4% and 81.5%, respectively. The input flat mirror M_1 was highly reflective (HR) coated at 639 nm and antireflective (AR) coated at the pump wavelength. The output coupler (OC) M_2 had radii of curvature of 200 mm with different transmittance of 1%, 2%, and 5% at 639 nm. In order to increase the heat dissipation effect, the crystal was wrapped in indium foil and mounted in a copper block cooled by the circulating

water at a temperature of 17 °C with temperature control precision of 0.1 °C. A KD*P crystal, a polarizer, and a quarter-wave plate together realized the Q-switched process. The polarizer coated for high transmittance at 639 nm was placed at Brewster angle in the cavity to select polarized light for oscillating. The widely used KD*P crystal (CPDPC-1020-2532-AR, COUPLETECH) with a dimension of Φ10 mm × 20 mm was employed as the EO switcher, which was AR coated at lasing wavelength. According to the calculation of EO Q-switched theory, the quarter-wave voltage was set at 1880 V.

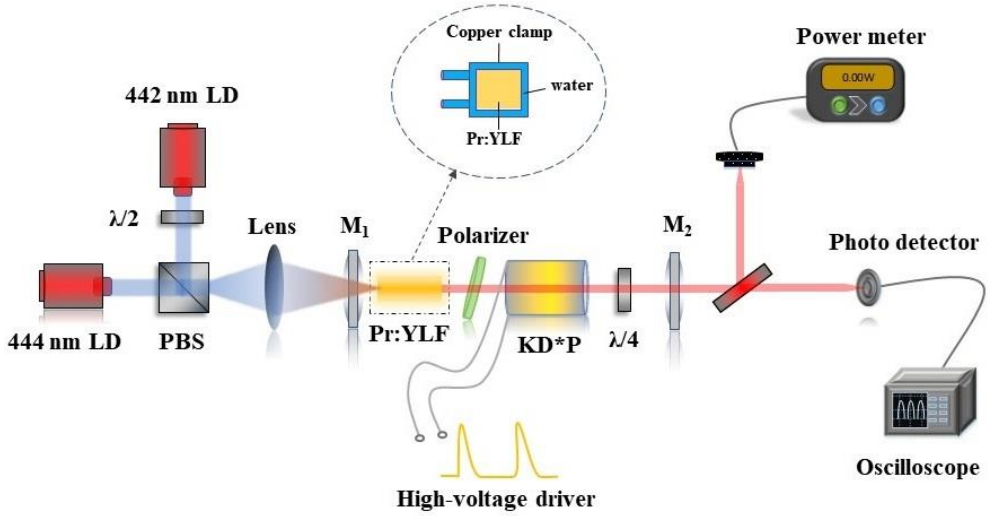

Fig. 1. Schematics of EO Q-switched Pr:YLF laser.

3. Results and discussion

At first, we studied the CW output performance of this laser without any inserting elements. A power meter (FieldMaxll-TO, COHERENT) was used to measure the laser output power. The CW Pr:YLF laser output characteristics with different OCs (T = 1%, 2%, and 5%) are shown in Fig. 2(a). A maximum CW output power of 1.55 W was achieved under the absorbed pump power of 3.97 W when an output coupler of T_{oc} = 5% was employed, corresponding to a slope efficiency of 44.2%. With the other OC transmissions, the maximum output powers declined to be 1.15 W (T = 1%) and 1.50 W (T = 2%), corresponding to slope efficiencies of 30.6% and 40.2%, respectively. To achieve optimal Q-switched output, the OC with the transmission of 5% was selected. When the polarizer, KD*P electro-optical crystal, and quarter-wave wave plate (static EO modulation) were inserted into the cavity orderly, the laser threshold increased and the output power decreased by comparison with the previous results, which was caused by insertion loss, also as shown in Fig. 2(a). The maximum average power of CW operation with inserting elements laser was 0.68 W at the absorbed pump power of 3.97 W, delivering the slope efficiency of 21.0%. The quarter-wave plate was rotated to restrain the laser oscillation. Then, the EO Q-switched operation was realized when the quarter-wave voltage was supplied to drive the KD*P crystal. The average output power of EO Q-switched laser versus the absorbed pump power with repetition rates ranging from 100 Hz to 500 Hz is presented in Fig. 2(b). The threshold absorbed pump power was 3.10 W, 3.10 W, 2.99 W, 2.99 W, and 2.99 W for the repetition rates of 100 Hz, 200 Hz, 300 Hz, 400 Hz, and 500 Hz, respectively. At the maximum absorbed pump power of 3.97 W, the maximum average output power at a repetition rate of 100, 200, 300, 400, and 500 Hz was 26, 29, 31, 33, and 34 mW, and the corresponding slope efficiency was 3.0%, 3.2%, 3.2%, 3.4%, and 3.5%, respectively. By optimizing the Q-switcher to increase the repetition frequency of the operation, the fluorescence efficiency of the EO Q-switched laser can be further improved in the future work. To investigate the stability of

the laser output, we recorded the maximum output power variation of EO Q-switched operation for 1 h, as shown in the inset of Fig. 2(b). The fluctuation of output power (output powers, rms) at the maximum absorbed pump power was measured to be 2.7%, 3.1%, 2.6%, 2.9%, and 2.8%, with different repetition rates of 100, 200, 300, 400, and 500 Hz, respectively. These results indicate that the laser cavity had high thermal stability. Fig. 3(a) shows the shortest pulse width achieved by EO Q-switched Pr:YLF laser with different modulation frequencies. The pulse width increased from 137 ns to 321 ns with the repetition rate from 100 Hz to 500 Hz. Figs. 3(b)-(c) show the tendency of corresponding pulse energy and peak power at a different repetition rate. The pulse energy decreased from 260 μJ to 68 μJ, and the peak power decreased from 1.90 kW to 0.21 kW. Under the repetition rate of 100 Hz, the output characteristics of the EO Q-switched laser are given in Fig. 4(a) and (b). As shown in Fig. 4(a) and (b), when the absorbed pump power increased from 3.10 W to 3.97 W, the pulse width decreased from 418 ns to 137 ns, the corresponding pulse energy increased from 10 μJ to 260 μJ, and the peak power increased from 0.02 kW to 1.90 kW. The output spectrum of the CW laser and EO Q-switched laser were recorded by the optical spectrum analyzer (MS 3504i), as shown in the inset of Fig. 4(b), which illustrated that the CW laser spectrum located at 639.5 nm with the full width at half maximum (FWHM) of 0.30 nm, while the EO Q-switched laser spectrum located at 639.4 nm with the FWHM of 0.26 nm. Compared to CW laser, the FWHM of the EO Q-switched laser spectrum became narrower and the center wavelength was slightly blue-shifted. The phenomenon may be caused by an insertion loss of EO modulator, which suppressed the laser mode with relatively small gain, thus induced spectrum narrowed and blue-shifted occurred.

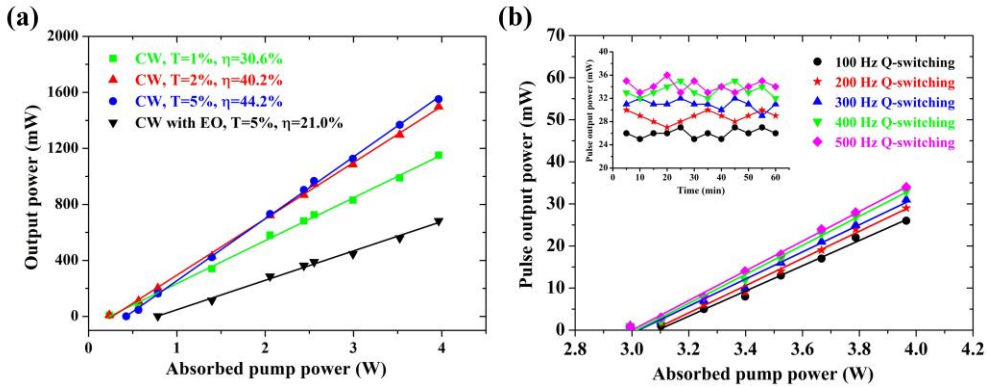

Fig. 2. (a) Output characteristics of CW and CW with EO Pr:YLF laser. (b) EO Q-switched output average power versus absorbed pump power at different repetition rates with T_{oc} =5%, the inset shows stability of EO Q-switched output power at different repetition rates.

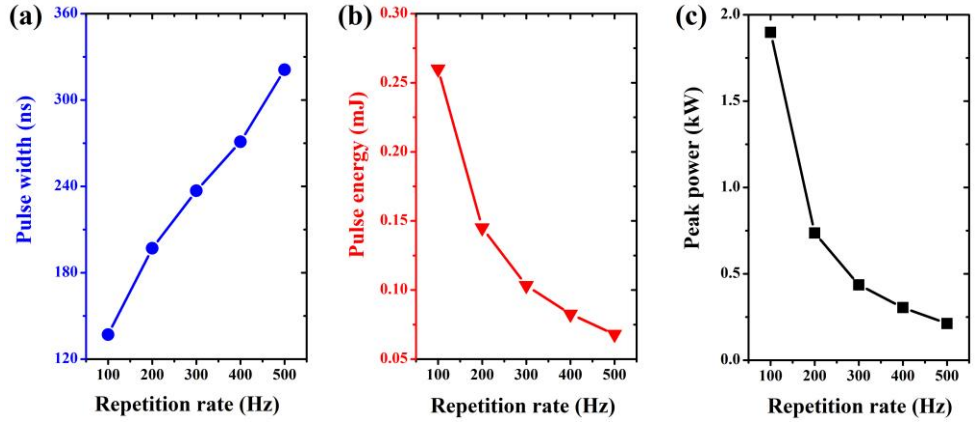

Fig. 3. (a) pulse width, (b) pulse energy, and (c) peak power versus repetition rates at the absorbed pump power of 3.97

W.

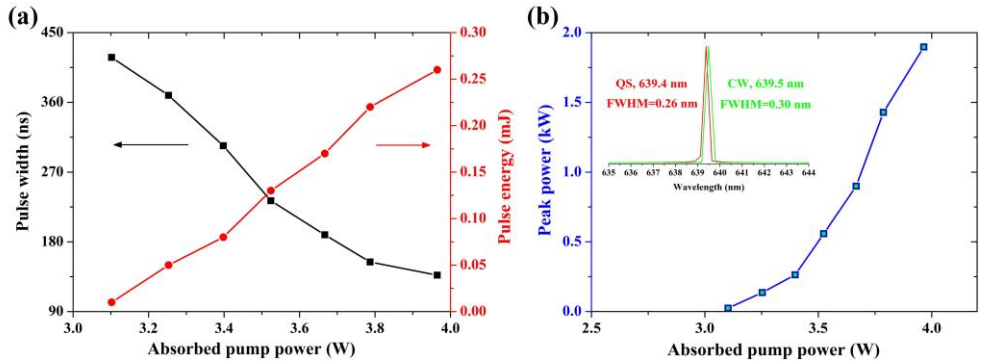

Fig. 4. (a) pulse widths and pulse energies of EO Q-switched laser versus absorbed pump power with a repetition rate of 100 Hz. (b) The calculated peak power, the inset shows the output spectra of CW laser and EO Q-switched laser.

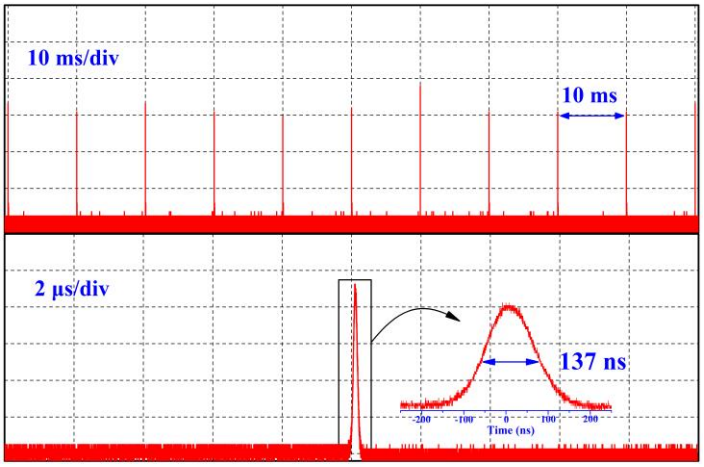

Fig. 5. The temporal pulse train and single pulse shape with a repetition rate of 100 Hz.

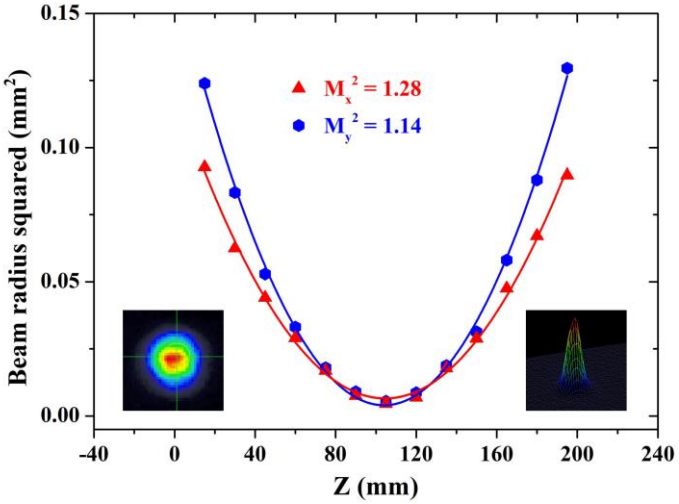

Fig. 6. Beam quality and spatial beam profile.

Under the maximum absorbed pump power of 3.97 W, the temporal pulse train and pulse shape of the shortest pulse duration at the repetition rate of 100 Hz were recorded by an oscilloscope (WAVESURFER 10, Teledyne LeCroy) and a fast photodetector (New Focus

1601), as shown in Fig. 5. The inset of Fig. 5 is the pulse profile with a pulse width of 137 ns. From the figure, it can be seen that the pulse profile was quite symmetrical, and there was no apparent streaking, which revealed the excellent performance of EO Q-switched output. A CCD camera (LaserCam HR II - 2/3", COHERENT) and a f = 100 mm of focal length lens were used to measure the output laser beam quality. The translation stage was moved along the straight line to record the beam radius of the tangential and the sagittal direction. According to the propagation law of the Gaussian beam, the beam quality of EO Q-switched laser with a repetition rate of 100 Hz under the condition of maximum output power was calculated as M_x^2=1.28, M_y^2=1.14, as shown in Fig. 6. Moreover, the laser beam profile and the three-dimensional light intensity map were also displayed in the insets of Fig. 6. The thermal effect partly deteriorated the beam quality of the Pr:YLF laser and can be further improved using more accurate compensation of the thermal lens effect, which is the cornerstone of our future work. For comparisons, the output performance of the ever obtained Pr-doped fluoride pulsed lasers at 639 nm based on different Q-switchers is summarized in Table 1. According to these results, EO Q-switched Pr:YLF visible laser exhibited excellent output characteristics. The repetition frequency of 100 Hz was lower than the Q-switched lasers in Table 1, but the corresponding pulse energy and peak power of EO Q-switched laser performed better than other works, almost three orders of magnitude larger than that of passively Q-switched Pr:YLF visible lasers which with Au nanorods [11], CQD [12], and $Ti_3C_2T_x$ [13] SAs. The results demonstrate the great potential of EO Q-switched visible laser to generate high energy laser pulses. The pulse width in this work was inferior to Co:MALO [14,15] and AO Q-switcher [16,17], but it was shorter than other passively Q-switched lasers in Table 1. In our work, the pulse width behaved an obvious shorten tendency with the increase in pump power, and we did not find any optical damage on the KD*P crystal. Due to the output capacity of the pump source, the pulse width of the output laser was limited to approximately 100 ns. If the power of pump source can be further increased, we believe the pulse width can be further compressed. In future, we will also try to increase the fluorescence efficiency of the laser by employing pulse pumping mode to improve the laser output efficiency. In addition, we will try to use LN or BBO as EO Q-switched crystal to realize the high repetition rate pulsed visible laser. In order to further increase the pulse energy of the output laser, the Pr-doped fluoride single crystal fiber [18] can be considered as the laser amplification medium to explore the practical route to realize the compact and high energy pulsed visible laser.

Table 1

Comparison of Pr^{3+}-doped pulsed red (639-640 nm) laser characteristics based on different Q-switchers.

Q-switcher	Repetition rate [kHz]	Pulse width [ns]	Pulse energy [μJ]	Peak power [W]	Ref.
Au nanorods	571	152	0.06	0.34	[11]
CQD	152.5	226	0.32	1.42	[12]
$Ti_3C_2T_x$	163	264	0.92	3.48	[13]
Co:MALO	64	30.9	33.5	1084	[14]
Co:MALO	780	8.5	1.3	140	[15]
AO	7.7	17	27	1570	[16]
AO	10	81.1	3.94	48.5	[17]
EO	0.1	137	260	1898	This work

4. Conclusions

In summary, characteristics of blue LD-pumped Pr:YLF visible laser running in EO Q-switched regime have been investigated. Under the absorbed pump power of 3.97 W, the Q-switched laser delivered the maximum pulse energy of 260 μJ, the highest peak power of 1.90 kW, and the shortest pulse width of 137 ns at a corresponding repetition rate of 100 Hz. This work indicates that EO Q-switched Pr:YLF laser can generate nanosecond pulses with kilowatt-level peak power, which well reveals an efficient way to promote the practical applications of the pulsed visible laser from rare-earth ions directly pumped by the blue laser diode.

Declaration of Competing Interest

The authors declare that they have no known competing financial interests or personal relationships that could have appeared to influence the work reported in this paper.

Acknowledgments

This work was supported by National Natural Science Foundation of China under Grant 12004208, Qilu University of Technology (Shandong Academy of Sciences) International Cooperation Project of Science, Education and Industry Integration and Innovation Pilot under Grant 2020KJC-GH12, National College Students Innovation and Entrepreneurship Training Program under Grant S202010431025.

References

1. K. V. Chellappan, E. Erden, H. Urey, Laser-based displays: a review, Appl. Opt. 49 (2010) F79-F98.
2. H. Pask, P. Dekker, R. Mildren, D. Spence, J. Piper, Wavelength-versatile visible and UV sources based on crystalline Raman lasers, Prog. Quantum Electron. 32 (2008) 121-158.
3. S. Calvez, J. Hastie, M. Guina, O. Okhotnikov, M. Dawson, Semiconductor disk lasers for the generation of visible and ultraviolet radiation, Laser Photonics Rev. 3 (2009) 407-434.
4. C. Kränkel, D. T. Marzahl, F. Moglia, G. Huber, P. Metz, Out of the blue: semiconductor laser pumped visible rare-earth doped lasers, Laser Photonics Rev. 10 (2016) 548-568.
5. D. T. Marzahl, P. W. Metz, C. Kränkel, G. Huber, Spectroscopy and laser operation of Sm^{3+}-doped lithium lutetium tetrafluoride ($LiLuF_4$) and strontium hexaaluminate ($SrAl_{12}O_{19}$), Opt. Express 23 (2015) 21118-21127.
6. H. Chen, H. Uehara, H. Kawase, R. Yasuhara, Efficient visible laser operation of Tb:$LiYF_4$ and $LiTbF_4$, Opt. Express 28 (2020) 10951-10959.
7. P. W. Metz, D. T. Marzahl, A. Majid, C. Kränkel, G. Huber, Efficient continuous wave laser operation of Tb^{3+}-doped fluoride crystals in the green and yellow spectral regions, Laser Photonics Rev. 10 (2016) 334-344.
8. G. Bolognesi, D. Parisi, D. Calonico, G. A. Costanzo, F. Levi, P. W. Metz, C. Kränkel, G. Huber, M. Tonelli, Yellow laser performance of Dy^{3+} in co-doped Dy,Tb:$LiLuF_4$, Opt. Lett. 39 (2014) 6628-6631.
9. A. Richter, E. Heumann, E. Osiac, G. Huber, W. Seelert, A. Diening, Diode pumping of a continuous-wave Pr^{3+}-doped $LiYF_4$ laser, Opt. Lett. 29 (2004) 2638-2640.
10. H. Tanaka, S. Fujia, F. Kannari, High-power visibly emitting Pr^{3+}:YLF laser end pumped by single-emitter or fiber-coupled GaN blue laser diodes, Appl. Opt. 57 (2018) 5923-5928.
11. S. X. Wang, Y. X. Zhang, J. Xing, X. F. Liu, H. H. Yu, A. D. Lieto, M. Tonelli, T. C. Sum, H .J. Zhang, Q. H. Xiong, Nonlinear optical response of Au nanorods for broadband pulse modulation in bulk visible lasers, Appl. Phys. Lett. 107 (2015) 161103.
12. B. Xu, S. Luo, X. Yan, J. Li, J. Lan, Z. Luo, H. Xu, Z. Cai, H. Dong, J. Wang, L. Zhang, CdTe/CdS Quantum Dots: Effective Saturable Absorber for Visible Lasers, IEEE J. Sel. Top. Quantum Electron. 23 (2017) 1-7.

13. Q. Yang, F. Zhang, N. Y. Zhang, H. Zhang, Few-layer MXene $Ti_3C_2T_x$ (T = F, O, or OH) saturable absorber for visible bulk laser, Opt. Mater. Express 9 (2019) 1795-1802.
14. S. Fujita, H. Tanaka, F. Kannari, Intracavity second-harmonic pulse generation at 261 and 320 nm with a Pr^{3+}:YLF laser Q-switched by a Co^{2+}:$MgAl_2O_4$ spinel saturable absorber, Opt. Express 27 (2019) 38134-38146.
15. M. Badtke, H. Tanaka, L. J. Ollenburg, S. Kalusniak, C. Kränkel, Passively Q-switched 8.5-ns Pr^{3+}:YLF laser at 640 nm, Appl. Phys. B: Lasers Opt. 127 (2021) 83.
16. J. Kojou, R. Abe, R. Kariyama, H. Tanaka, A. Sakurai, Y. Watanabe, F. Kannari, InGaN diode pumped actively Q-switched intracavity frequency doubling Pr:$LiYF_4$ 261 nm laser, Appl. Opt. 53 (2014) 2030-2036.
17. L. Jin, W. C. Dai, Y. J. Yu, Y. Dong, G.Y. Jin, Single longitudinal mode Q-switched operation of Pr:YLF laser with pre-lase and Fabry-Perot etalon technology, Opt. Laser Technol. 129 (2020) 106294.
18. A. Sottile, Z. Zhang, S. Veronesi, D. Parisi, A. Di Lieto, M. Tonelli, Visible laser operation in a Pr^{3+}:$LiLuF_4$ monocrystalline fiber grown by the micro-pulling-down method, Opt. Mater. Express 6 (2016) 1964-1972.